Staging cerebral amyloid angiopathy: from marker to model

Koemans, E.A.

4

SEX DIFFERENCES IN HISTOPATHOLOGICAL MARKERS OF CEREBRAL AMYLOID ANGIOPATHY AND RELATED HEMORRHAGE

Chapter 4 | Sex differences in histopathological markers of cerebral amyloid angiopathy and related hemorrhage

E.A. Koemans[1,2,4], V. Perosa[2], W.M. Freeze[1], H. Lee[4], M.G. Kozberg[2,3], G. Coughlan[2], R.F. Buckley[2], M.J.H. Wermer[1,5], S.M. Greenberg[2], S.J. van Veluw[2,3,6]

[1] *Department of Neurology, Leiden University Medical Center, Leiden, The Netherlands.*

[2] *Department of Neurology, Massachusetts General Hospital, Harvard Medical School, Boston, MA, USA.*

[3] *MassGeneral Institute for Neurodegenerative Disease, Massachusetts General Hospital, Harvard Medical School, Charlestown, MA, USA.*

[4] *Department of Biostatistics, Massachusetts General Hospital, Harvard Medical School, Boston, MA, USA.*

[5] *Department of Neurology, University Medical Center Groningen, Groningen, The Netherlands*

[6] *Department of Radiology, Leiden University Medical Center, Leiden, The Netherlands.*

Submitted

Abstract

Background: Men with cerebral amyloid angiopathy (CAA) may have an earlier onset of intracerebral hemorrhage and a more hemorrhagic disease course compared to women. Here, we investigated sex differences in histopathological markers associated with amyloid-β burden and hemorrhage in cognitively impaired individuals and patients with CAA, using neuropathological data from two autopsy cohorts.

Methods: First, we assessed presence of parenchymal (Thal score) and vascular amyloid-β (CAA severity score) in cognitively impaired individuals from the National Alzheimer's Coordinating Center (NACC) neuropathology database, using generalized estimating equations (GEE). Next, we explored sex differences in hemorrhagic ex vivo MRI-markers and local cortical iron burden, and the interaction of sex on factors associated with cortical iron burden (CAA percentage area and vessel remodelling) in participants with pathologically confirmed clinical CAA from the Massachusetts General Hospital (MGH) CAA database, using Poisson regression, linear mixed effects models, and deep-learning derived measures for CAA and iron.

Results: In 6120 participants from the NACC-database (45% women, mean age 80y), we found a lower probability of parenchymal amyloid-β presence in men (OR [95%CI]=0.68 [0.53-0.88]) but no sex difference in vascular amyloid-β presence relative to women. In 19 patients with definite CAA from the MGH-database (35% women, mean age 75y), we found a lower microbleed count ($p<0.001$), but a higher proportion of cortical superficial siderosis and a higher local cortical iron burden in men ($p<0.001$). CAA percentage area was comparable in men and women ($p=0.732$). Exploratory analyses demonstrated a possible stronger negative relation between cortical CAA percentage area and cortical iron density in men compared to women ($p=0.03$).

Conclusion: Previously observed sex differences in hemorrhage onset and progression in CAA patients are likely not due to differences in global CAA severity between men and women. Other factors, such as vascular remodelling, may contribute, but future studies are necessary to replicate our findings in larger datasets and to further investigate the underlying mechanisms behind these complex sex differences.

Introduction

Cerebral amyloid angiopathy (CAA) is one of the leading causes of lobar intracerebral hemorrhage (ICH), and a major contributor to vascular dementia in the elderly.[1] CAA is characterized by the gradual deposition of the protein amyloid-β in the walls of cortical and leptomeningeal arteries of the brain, which eventually leads to hemorrhage.

Accumulating evidence suggests that hemorrhages occur in the final stages of CAA disease [2-4] Insights from histopathological and pre-clinical studies using mouse models show that amyloid-β initially deposits in the basement membranes surrounding vascular smooth muscle cells, leading to loss of smooth muscle, thickening of the vessel wall, and eventually vessel wall remodelling.[2, 3, 5, 6] Two types of remodelling have been described: Vonsattel grade III vessel remodelling, a concentric splitting of the vessel wall (also called 'vessel-within-vessel' appearance) often seen in leptomeningeal arterioles and presumed to be related to cortical superficial siderosis (cSS), and Vonsattel grade IV vessel remodelling, characterized by loss of amyloid-β locally with replacement of the arteriolar wall with fibrinoid material, more rarely seen and thought to underly microbleed formation.[2, 3, 5, 7]

Patients with CAA show a striking variability in onset and disease course.[8, 9] This variability is also present in individuals with hereditary Dutch-type CAA (D-CAA), an autosomal dominant variant of CAA which is often seen as a relatively pure, genetic model for the disease.[10] A previous study from our group suggested that biological sex moderates the presentation of CAA and contributes to variability in onset and disease course. Specifically, male sex was associated with an earlier age of first ICH in sCAA. a higher number of ICH recurrences in D-CAA and a higher microbleed count in sporadic CAA (sCAA).[11]

Based on the literature mentioned above, we hypothesize two possible pathophysiological mechanisms that may underly these observed sex differences: first, sex may influence global amyloid-β load, resulting in men having earlier or more severe amyloid-β deposition compared to women, which would increase bleeding risk or onset. Second, sex might influence factors leading to bleeding after vascular amyloid-β accumulation, such as vessel remodelling, resulting in men to have a more hemorrhagic CAA phenotype compared to women. With these hypotheses in mind, we explored sex differences in histopathological markers of amyloid-β and hemorrhage in CAA using two different autopsy cohorts.

Methods

NACC database

Participants

In the first part of this study, we investigated sex differences in presence of vascular and parenchymal amyloid-β deposition in cognitively impaired autopsied individuals, using data from the National Alzheimer's Coordinating Center (NACC) neuropathology database. Use of these data for this specific project was granted on April 29th, 2022. The NACC database contains longitudinal clinical and neuropathological data from participants collected via National Institute on Aging funded Alzheimer's Disease Research Centers (ADRCs) across the United States since 2005, with different underlying etiologies including Alzheimer's disease and Parkinson's disease as well as healthy individuals. [12] Informed consent was obtained from all participants or next of kin prior to study enrolment, and the study was approved by the local institutional review boards of each participating institution. The database contains coded demographics, clinical data (including physician diagnosis of hypertension and hypercholesterolemia), genetic data (including *APOE*-ε4 status, a known risk factor for CAA and Alzheimer's disease) and neuropathology data obtained after autopsy (including CAA severity score for vascular amyloid-β and Thal score for parenchymal amyloid-β). [12] The database includes participants with normal cognitive function, as well as three stages of cognitive impairment: subjective impaired cognition, mild cognitive impairment (MCI), and dementia. We selected only individuals aged ≥ 50 years at time of death and excluded those with a diagnosis of normal cognition at the last visit before autopsy.

Immunohistochemistry against amyloid-β was applied using different antibodies. In the registry, vascular amyloid-β indicating CAA severity was measured using a semi-quantitative scale adapted from prior studies. [5, 13] CAA burden was described as 0 = absent, 1 = mild (scattered positivity in parenchymal and/or leptomeningeal vessels), 2 = moderate (intense positivity in many parenchymal and/or leptomeningeal vessels), 3 = severe (widespread [more than one brain area] intensive positivity in parenchymal and leptomeningeal vessels). [5] Parenchymal amyloid-β (plaque burden) was scored according to Thal score, a previously published system which distinguishes 4 phases of amyloid-β plaque severity according to anatomical progression: A0 = no amyloid-β; A1 = isocortical amyloid-β and/or limbic amyloid-β; A2 = basal ganglia amyloid-β; A3 = basal forebrain and midbrain amyloid-β, and/or pons/medulla oblongata and cerebellum amyloid-β. [14, 15]

MGH CAA pathology database

Participants

In the more exploratory second part of this study, we aimed to investigate the hypothesis that men with CAA have a more hemorrhagic phenotype compared to women. Firstly, we investigated sex differences in hemorrhagic MRI markers (macrobleeds, microbleeds, and cSS) on ex vivo 3 tesla MRI between men and women. Secondly, we investigated sex differences in density of cortical iron deposition, a quantitative measure derived from deep learning-based models, [16] which was operationally defined as a proxy for cumulative local hemorrhage severity. [17] Although cortical iron density can be considered a measure of all hemorrhagic lesions (microbleeds, macrobleeds, and cSS), our work suggests that iron density predominantly reflects cSS severity. [2, 16 17] We further explored sex differences in CAA by taking into account previously investigated factors associated with hemorrhage (and therefore likely contributing to cortical iron deposition): cortical and leptomeningeal CAA area percentage and degree of leptomeningeal vessel wall remodelling (Vonsattel grade III). [2, 5, 7]

We investigated our hypotheses using autopsy data from patients with a pathologically confirmed clinical diagnosis of CAA, collected at Massachusetts General Hospital (MGH). This database is part of a program initiated in 2015 within the hemorrhagic stroke research program, which aims to study the neuropathological correlates of MRI manifestations of CAA. The program has been approved by the MGH institutional review board (2021P001920) and informed consent was obtained prior to autopsy from brain donors next of kin or other legal representatives. The process of autopsy data collection is described in previously published works. [7,10,11] To summarize: after autopsy one formalin-fixed hemisphere underwent routine neuropathological examination by a board-certified neuropathologist, whereas the other, most intact, formalin-fixed hemisphere was subjected to ex vivo 3 tesla MRI and histopathological examination. The single-hemisphere ex vivo MRI scans were visually assessed for CAA-related MRI markers (macrobleeds, microbleeds, cSS), defined according to the Standards for Reporting Vascular Changes on Neuroimaging (STRIVE) criteria, as previously reported. [2, 3, 18, 19]

Histopathology

Details regarding the preparation of the histopathologic samples can be found in previous publications from our group. [2, 3, 19] To summarize: samples from pre-defined areas of the brain were cut from 1cm thick coronal slabs (frontal, temporal,

parietal, and occipital). Blocks were processed and embedded in paraffin, after which 6-µm thin sections were cut using a microtome. Haematoxylin and eosin (H&E) and Perls' Prussian blue staining were performed according to standard histology protocols. For the Perls' protocol, sections were incubated using a 1:1 mixture of 5% hydrochloric acid and 5% potassium ferrocyanide for 30 minutes, and afterwards counterstained with filtered neutral red for 1 min.[2] Immunohistochemistry was performed against amyloid-β as previously described on adjacent sections.[2, 3, 19] The stained sections were scanned using a Hamamatsu Nano-Zoomer Digital Pathology (NDP)-HT whole slide scanner (C9600-12, Hamamatsu Photonics KK, Japan), at 20 × magnification. Quantitative measures for CAA (cortical and leptomeningeal) and density of iron-positive deposits in the cortex were obtained, as detailed in previous publications from our group, using deep-learning based models built within the Aiforia® platform.[16, 19] The following parameters were calculated: percentage of leptomeningeal CAA area (leptomeningeal CAA area [mm^2]/leptomeningeal tissue area [mm^2]); percentage of cortical CAA area (cortical CAA area [mm^2]/cortical tissue area [mm^2]); density of iron positive deposits/mm^2 cortex (Total count of iron deposits/cortex area [mm^2]) (Figure 1).[19] Calculations were performed separately for each individual brain region (frontal, parietal, temporal, occipital). For descriptive statistics, mean quantitative scores for the whole brain were obtained in the following way: added total scores of all brain regions/number of brain regions. We used existing data in which the degree of leptomeningeal grade III vessel remodelling was quantified. For each brain region, the degree of leptomeningeal grade III vessel wall remodelling was determined according to the following score: 0 = absent, 1 = occasional vessel, 2 = many vessels (Figure 1).[2] For descriptive statistics, a total leptomeningeal grade III vessel wall remodelling score was calculated for each individual by adding the scores of the four brain regions to create a score between 0-8. We investigated the leptomeningeal grade III remodelling as previous studies have shown that it is strongly associated with blood-brain barrier leakage and hemorrhage (cSS and ICH) in CAA.[2, 3, 5, 7, 20] Unfortunately, we could not investigate the effect of (parenchymal) grade IV vessel remodelling: whereas grade III vessel remodelling was often seen and could be categorised in leptomeningeal tissue of our participants with CAA, grade IV vessel remodelling was seen very rarely, and therefore, the counts of grade IV vessel remodelling in our cohort were too low to be included in the analyses.[2, 3, 7]

Statistics

NACC database

We performed statistical analysis using the software R studio, version 3.6.0 (R Foundation for Statistical Computing, Vienna, Austria; www.R-project.org) and the Statistical Package for Social Science (IBM SPSS Statistics), version 26. We used package 'gee' for R statistical software. We used descriptive statistics to analyse baseline characteristics. To investigate sex differences in vascular amyloid-β (CAA severity score) and parenchymal amyloid-β (Thal phase) we applied generalized estimating equations (GEE) for logistic regression, all corrected for age at death. We assumed a logit link function for binary outcome with an independent correlation structure to account for within-center correlation (GEE). As we expected a relatively low sample size of participants with CAA, we transformed the categorical global CAA burden score into a binary variable: absent versus present (CAA severity mild/moderate/severe). In sensitivity analysis, we repeated the analysis using a modified variable (absent-mild CAA versus moderate-severe CAA), and by transforming Thal phase into a binary variable (absent (A0) versus present (A1/A2/A3)). Given the significant contribution of age and *APOE*-ε4 status (dichotomized as presence of at least 1 ε4 allele vs none) on parenchymal amyloid burden we corrected these in all models. In the model using CAA as a dependent variable, we additionally corrected for Thal phase to investigate a possible confounding effect. In exploratory *Post-hoc analyses*, we fitted a second model for both outcomes, in which we additionally corrected for presence of cardiovascular risk factors (hypertension and hypercholesterolemia). Furthermore, we explored sex-differences in CAA severity and Thal phase using the outcomes as ordinal variables. We assumed a cumulative logit link function for ordinal outcome, again with an independent correlation structure to account for within-center correlation. An $\alpha<0.05$ was considered statistically significant and all p-values are two-tailed.

MGH CAA pathology database

We used descriptive statistics to calculate baseline characteristics. First, we investigated sex-differences in hemorrhagic lesions at ex vivo single-hemisphere 3 tesla MRI. We investigated sex differences in macro- and microbleed count and cSS frequency using Poisson regression analysis, corrected for age at death, to obtain adjusted relative risks (aRR) with 95%CI. Second, we investigated sex differences in total CAA percentage area, cortical iron density (as a measure for hemorrhage load but mostly reflecting cSS), again using Poisson regression analysis corrected for age

at death. To explore the association between male sex and cortical iron density we fitted linear mixed effects (LME) models using the package 'lme4' in R. All models contained density of iron positive deposits/mm^2 cortex as a dependent variable, and subject ID and cortical region as random factors to account for subject- and region- dependent differences. Age at death was included as covariate in the model. First, we fitted the null model which included age at death and sex. Secondly, we fitted three sets of models: a first model with leptomeningeal grade III vessel wall remodelling and sex as interaction factor, a second model with leptomeningeal CAA area and sex as interaction factor, and a third model with cortical CAA area and sex as interaction factor (Table 4). Models were compared using likelihood ratio tests, and ANOVA tests were used to compare the individual models to the null model. Lastly, we fitted a comprehensive model including all independent variables which showed a significant association with cortical iron density in prior analyses. We plotted scatterplots to illustrate the relation between leptomeningeal grade III vessel remodelling and iron density, and cortical CAA area percentage and iron density, stratified by sex, and visually checked for outliers. An $\alpha<0.05$ was considered statistically significant. All reported p-values are two-tailed.

Results

NACC database

We included 6120 participants with autopsy data from the NACC database, 3370 (55%) men and 2750 (45%) women, mean age at death 81 years (range 50-111) (Table 1).

The GEE analysis investigating sex differences in presence of vascular amyloid-β(CAA) contained 2844 individuals. Presence of vascular amyloid-β indicative of CAA did not differ between men and women (OR [95%CI] = 1.05 [0.87-1.27]), correcting for age, APOE and Thal stage. The GEE analysis investigating sex differences in the presence of parenchymal amyloid-β (Thal phase) contained 2854 individuals. Men were less likely to have parenchymal amyloid-β in the cortex (i.e. Thal score>A0) compared with women (OR [95%CI] = 0.68 [0.53-0.87]). The outcomes did not change when using ordinal regression investigating sex differences in CAA severity score or Thal score (as categorical variables) instead of logistic regression, nor did the outcomes change when investigating absent-mild CAA versus moderate-severe (Table 2). Correction for history of hypercholesterolemia and hypertension also did not change the outcomes (Table 2).

Table 1: Baseline characteristics of NACC database participants with available neuropathology data.

	All (n=6120)	Males (n=3370)	Females (n=2750)
Mean age at death in years (range)	80 (50-111)	78 (50-110)	81 (50-111)
Mean interval between last UDS visit and death in months (range)	20 (0-161)	18 (0-152)	22 (0-161)
APOE-ε4[1]			
One ε4 allele (n, %)	2048 (34)	1114 (33)	934 (34)
Two ε4 alleles (n, %)	504 (8)	285 (9)	219 (8)
Hypertension (n, %)[2]	848 (14)	459 (14)	389 (14)
Hypercholesterolemia (n, %)[3]	805 (13)	469 (14)	336 (12)
CAA pathology at autopsy[4]			
None (n, %)	2266 (37)	1278 (38)	988 (36)
Mild (n, %)	1722 (28)	926 (28)	796 (29)
Moderate (n, %)	1295 (21)	697 (21)	598 (22)
Severe (n, %)	707 (12)	402 (12)	305 (11)
Thal phase at autopsy[5]			
A0 (n, %)	384 (6)	245 (7)	139 (5)
A1 (n, %)	410 (7)	237 (7)	173 (6)
A2 (n, %)	360 (6)	188 (6)	172 (6)
A3 (n, %)	2125 (35)	1104 (33)	1021 (37)

[1]Missing/unknown n=737; [2]Missing/unknown n=4385; [3]Missing/unknown n=4414; [4]Missing/unknown n=130; [5]Missing/unknown n=2841.

MGH CAA pathology database

We included 19 patients with definite CAA (mean age at death 75 years, 7 [35%] women) (Table 3). Men had lower microbleed counts on ex vivo MRI compared to women (median 109 vs. 45; aRR 0.39, p<0.001), whereas men numerically had more often cSS on ex vivo MRI compared with women (67% vs. 29%, aRR -0.91, p=0.25). On neuropathology, men had a higher local cortical iron density compared to women (median 6.42/mm2 vs. 5.13/mm2, aRR -0.75, p<0.001), which is consistent with an overall increased cSS burden in men. Total CAA percentage area was comparable between men and women (median 1.32 vs. 1.20; aRR -0.15, p=0.73).

Table 2: GEE parameter estimates on both the logit and odds-ratio scale.

	Vascular amyloid-β (CAA severity score) (n=2844)		Parenchymal amyloid-β (Thal score) (n=2854)	
	B (SE)	*OR [95%CI]*	*B (SE)*	*OR [95%CI]*
Male sex[1,2]	0.051 (0.096)	1.052 [0.872-1.269][3,4]	-0.386 (0.128)	0.680 [0.528-0.876]*[5]
Age at death	0.003 (0.004)	1.003 [0.995-1.012]	0.039 (0.006)	1.040 [1.028-1.052]*
APOE-ε4 status positive	0.918 (0.099)	2.505 [2.065-3.039]*	2.540 (0.203)	12.68 [8.512-18.890]*
Thal phase A1	1.785 (0.246)	5.958 [3.677-9.655]*	X	X
Thal phase A2	2.627 (0.255)	13.837 [8.395-22.811]*	X	X
Thal phase A3	3.631 (0.230)	37.764 [24.083-59.218]*	X	X

*B: raw parameter estimate (on logit scale); SE: robust (sandwich) standard error; OR: odds ratio; 95%CI: 95% confidence interval. *statistically significant (p<0.05).*

[1]Modifying the analysis to compare CAA stage non-mild versus moderate-severe did not change the model outcomes (effect male sex on CAA: OR [95%CI]: 1.049 [0.887-1.241].

[2]Analysis using ordinal regression with CAA severity score and Thal phase as ordinal dependent variables in the GEE model did not change the model outcomes (effect male sex on CAA: OR [95%CI]: 1.080 [0.911-1.280], effect male sex on Thal phase: OR [95%CI]: 0.810 [0.701-0.937]).

[3]Running the model without including Thal stage as a factor did not change the model outcomes (effect male sex on CAA: OR [95%CI] 1.000 [0.887-1.127]

[4]Adding possible confounders hypertension and hypercholesterolemia to the model did not change the model outcome but did drastically decrease the sample size (OR [95%CI]: 1.118 [0.867-1.441], n=1481).

[5]Adding possible confounders hypertension and hypercholesterolemia to the model did not change the model outcome but did drastically decrease the sample size (OR [95%CI]: 0.679 [0.479-0.962], n=1487).

Next, we explored the relation between sex and cortical iron density in further detail using LME models. The model included all 19 cases, together a total of 71 sections (5 sections were excluded because of inaccurate detections by the Aiforia® algorithm). Results of the models are described in detail in Table 4. The variables that showed a significant main association with cortical iron density were leptomeningeal vessel remodelling, in model 1 and 4 (a positive association) and cortical CAA area percentage, in model 4 (a negative association).

Figure 1: Examples of iron deposits in the cortex, cortical and leptomeningeal CAA and leptomeningeal grade III vessel remodelling.

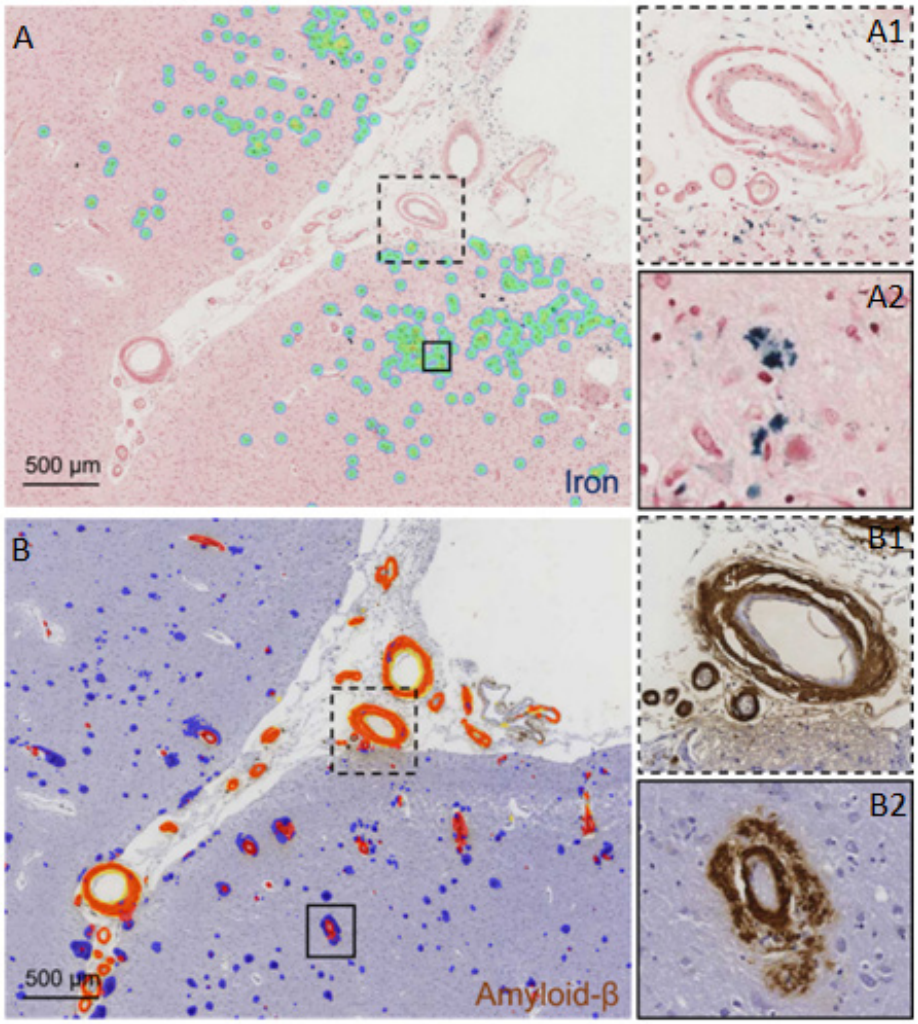

Examples of the application of a deep learning model (Aiforia ®) for iron (A) and amyloid (B) in two adjacent brain sections of a participant with CAA. A: Cortical iron deposits recognized by the model are overlaid in green (stained blue, see corresponding inset A2). B: parenchymal amyloid recognized by the model is overlaid in blue, CAA (cortical and leptomeningeal) recognized by the model in red (see corresponding inset B1 and B2, amyloid stained brown). Inset A1 and B1 shows an example of a single leptomeningeal vessel with Vonsattel grade III remodelling (vessel-in-vessel pathology). The inset B2 shows an example of a cortical vessel with dyshoric CAA.

Table 3: MGH CAA pathology cohort.

	Total (n=19)	Males (n=12)	Females (n=7)	aRR (95%CI) [p-value]
Mean age at death in years (range)	75 (65-89)	74 (65-86)	76 (65-89)	-
Ex vivo 3 tesla MRI (single hemisphere)				
Macrobleed prevalence (%)	11 (58)	6 (50)	5 (71)	-
Median macrobleed count (range)	1 (0-5)	0.5 (0-5)	2 (0-3)	0.44 (-0.35-1.22) [0.261]
Microbleed prevalence (%)	10 (100)	12 (100)	7 (100)	-
Median microbleed count (range)	49 (4-261)	45 (4-261)	109 (9-204)	**0.39 (0.29-0.49) [<0.001]**
cSS (n, %)	10 (53)	8 (67)	2 (29)	-0.91 (-2.8-0.49) [0.253]
Histopathology				
Median count of iron deposits/mm^2 in cortex (range)1	5.34 (0.29-71.80)	6.42 (0.73-71.80)	5.13 (0.27-14.78)	**-0.75 (-1.11- -0.41) [<0.001]**
Median Total CAA area (%, range)[1]	1.26 (0.40-2.71)	1.32 (0.40-2.71)	1.20 (0.72-1.63)	-0.15 (-1.04 -0.67) [0.732]
Median Cortical CAA area (%, range)[1]	0.78 (0.26-1.44)	1.01 (0.26-1.44)	0.75 (0.39-1.12)	-
Median Leptomeningeal CAA area (%, range)[1]	28.30 (8.89-57.90)	19.88 (8.88-57.90)	41.11 (15.69-46.09)	-
Median leptomeningeal vessel wall remodelling score[2] (range)	4 (0-8)	5 (0-8)	3 (1-7)	-

[1]*All scores for whole brain obtained by adding regional scores and dividing by number of regions used.*
[2] *Scores per region added to create a score for whole brain between 0-8.*
Significant effects are highlighted in **bold**.

Table 4: LME investigating sex differences in factors influencing cortical iron density.

	(0) M0	(1a) with leptomeningeal vessel remodelling	(1b) with leptomeningeal vessel remodelling interaction with sex	(2a) with leptomeningeal CAA area (%)	(2b) with leptomeningeal CAA area (%):sex	(3a) with cortical CAA area (%)	(3b) with cortical CAA area (%):sex	(4 comprehensive model
Age at death (y)	P=0.231 estimate= -0.541 (-1.412-0.432)[1]	P=0.143 estimate= -0.6241 (-1.468-0.218)	P=0.114 estimate= -0.649 (-1.458-0.159)	P=0.154 estimate= -0.640 (-1.525-0.255)	P=0.094 estimate= -0.740 (-1.596-0.135)	P=0.182 estimate= -0.577 (-13.108-3.392)	P=0.199 estimate= -0.522 (-1.331-0.2888)	P=0.111 estimate= -0.613 (-1.368-0.144)
Sex (male 0, female 1)	P=0.473 estimate= -5.252 (-2.080-0.886)[1]	P=0.646 estimate= -3.147 (-17.012-10.728)	P=0.592 estimate= 4.437 (-12.391-20.779)	P=0.423 estimate= -5.667 (-19.876-8.667)	P=0.505 estimate= 9.272 (-19.172-36.698)	P=0.415 estimate= -5.687 (-19.679-8.476)	**P=0.038 estimate= - 18.958 (-36.549- - 0.832)**	P=0.102 estimate= -14.236 (-31.180-3.315)
Leptomeningeal grade III vessel remodelling		**P=0.005 estimate= 7.189 (2.324-12.059)**	**P=0.002 estimate= 9.735 (3.853-15.618)**					**P=0.008 estimate= 6.545 (1.749-11.335)**
Leptomeningeal grade III vessel remodelling: sex			P=0.139 estimate= -7.686 (-18.034-2.609)					
Leptomeningeal CAA area (%)				P=0.299 estimate= 0.170 (-0.164-0.492)	P=0.115 estimate= 0.303 (-0.091-0.676)			
Leptomeningeal CAA area (%):sex					P=0.222 estimate= -0.434 (-1.133-0.287)			
Cortical CAA area (%)						P=0.235 estimate= -4.733 (-13.108-3.392)	**P=0.022 estimate= - 11.352 (-21.378- -1.384)**	**P=0.028 estimate= - 10.362 (-20.040- - 0.752)**
Cortical CAA area (%):sex							**P=0.034 estimate= 17.191 (1.351-33.279)**	*P=0.084 estimate= 13.516 (-1.97-29.276)*

	(0) M0	(1a) with leptomeningeal vessel remodelling	(1b) with leptomeningeal vessel remodelling interaction with sex	(2a) with leptomeningeal CAA area (%)	(2b) with leptomeningeal CAA area (%):sex	(3a) with cortical CAA area (%)	(3b) with cortical CAA area (%):sex	(4 comprehensive model
Log likelihood	-284.0	-279.9	-278.9	-283.5	-282.8	-283.4	-281	-278
AIC	580	574	573	581	582	580	578	573
BIC	593	589	591	597	599	596	596	593
Anova outcome (m0,…)		**0.004364**	0.141242	0.3066	0.2307	0.2521	**0.03377**	**0.005082**

Results for the fixed effects of linear mixed effects models looking at the influence of sex on cortical iron density. Subject and cortical region (frontal, temporal, parietal, occipital) were set as random factors for the intercept. Data represent standardized fixed effects estimates with confidence intervals and statistical significance. Models were compared using likelihood ratio tests; smaller AIC and BIC values indicate a better model fit. Significant effects are highlighted in ***bold****, trend towards significance in italics.*

[1]*95%CI obtained via bootstrapping.*

To visualise our data, we plotted scatterplots for the relation between cortical CAA area percentage and cortical iron density, and leptomeningeal grade III vessel remodelling and cortical iron density, for men and women (Figure 2). The scatterplots suggested an opposite relation of cortical CAA area percentage with cortical iron density in men and women (Figure 2A, Table 1 of supplementals). This interaction effect of sex was statistically significant (p=0.034, model 3b), suggesting sex moderates this relationship. This significance became attenuated in a more comprehensive model 4 (p=0.08). Leptomeningeal CAA area percentage was not associated with cortical iron density, nor was there an interaction effect of sex.

Figure 2: Scatterplots illustrating cortical iron density against leptomeningeal grade III vessel remodelling score and against cortical CAA area percentage in males and females.

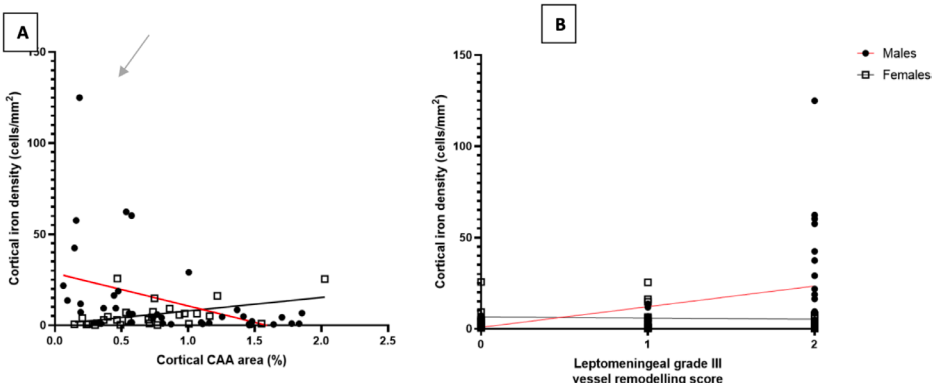

Scatterplots of n=19 cases (71 sections) illustrating: (A) the relation between cortical iron density and cortical CAA area in males (black circles) and females (hollow squares) with simple linear regression lines to estimate direction (males red line, females black line). (B) the relation between cortical iron density and leptomeningeal grade III vessel remodelling score in males (black circles) and females (hollow squares), with simple linear regression lines to estimate direction (males black line, females red line). In both scatterplots the (same) outlier can be seen, a single brain section in a male participant (grey arrows). After exclusion of this outlier all previously found significant associations remained stable, increasing in significance (Supplemental Table 1). A stronger association of leptomeningeal grade III vessel remodelling with cortical iron density compared to females was observed after exclusion of the outlier (Supplemental Table 1).

Discussion

In this study, we explored sex differences in CAA histopathology. In an autopsy cohort of cognitively impaired individuals, women exhibited a higher prevalence of parenchymal amyloid-β (Thal staging) compared to men. In contrast, no sex

differences were observed in the presence of vascular amyloid-β (CAA). In a different cohort of patients with neuropathologically confirmed CAA, we found significantly more microbleeds on ex vivo MRI in women, but a significantly higher local cortical iron burden – in line with increased cSS – in men. Total CAA percentage area was comparable between men and women in this dataset. Exploratory analyses suggested that the strongest contributing factor to local cortical iron burden was leptomeningeal grade III vessel remodelling. Furthermore, we found that higher cortical CAA area percentage was related to a lower cortical iron density, and that sex moderated this association, such that the association was stronger in men compared to women.

The finding that female sex is related to higher parenchymal amyloid-β prevalence is consistent with previous studies, which found that women exhibit elevated Alzheimer's disease pathology, compared to age-matched men. [21, 22] Our results were inconsistent with a similar autopsy study performed in participants with Alzheimer's disease, which demonstrated that men have higher vascular CAA severity scores compared to women. [23] This discrepancy might be due to a difference in CAA severity categorization between this study and the NACC database. Furthermore, the NACC database contains a larger but more heterogenous population, whereas the previous study used autopsy data of individuals with neuropathologically-confirmed Alzheimer's disease. Based on our current observations, it seems unlikely that the previously identified differences in ICH onset and recurrence between men and women with CAA can sufficiently be explained by differences in global CAA severity between both sexes. [11]

On ex vivo MRI, we found higher microbleed counts in women compared to men. This is inconsistent with our previous *in-vivo* study that demonstrated that men had a higher prevalence and count of microbleeds. Similarly, these ex-vivo results contradict a previous in-vivo study in Alzheimer's disease which also found higher lobar microbleed counts in men compared to women. [11, 24] We speculate these discrepancies might be due to the differences in sample size, as well as the differences in disease stage (the MGH autopsy dataset being an end-stage cohort by design).

We next explored sex differences in cortical iron burden, which was higher in men compared to women. Since local iron burden as measured here predominantly reflects cSS, this effect is likely driven by the fact that men in this cohort more often had cSS compared to women. [2, 16]

We furthermore explored the possible interaction effect of sex on factors contributing to cortical iron burden. We observed a negative association of local cortical CAA area percentage with local cortical iron density. This is in line with previous observations in the same cohort, where we found a strong relationship between increased leptomeningeal CAA severity and cSS in the form of local iron burden, and a negative

association between cortical CAA severity and local iron burden.[2] It is intriguing that our data (Figure 2A) suggest that this negative association is more apparent in men than in women with CAA, although men had fewer microbleeds compared to women. This again may be because in the men of our population, cSS is probably the major contributing factor to the local cortical iron burden, and cSS is not associated with cortical CAA.[2] The previously observed relationship between leptomeningeal CAA area percentage and cortical iron burden could not be confirmed, possibly because of the inclusion of additional cases between the prior study and now.[2]

This study has several limitations. Firstly, the NACC data collection is not population-based. Therefore, the data are heterogeneous and subject to enrolment bias. The heterogeneity makes results more generalizable to a general population, however it does lead to relatively 'low' prevalence of CAA. Furthermore, the NACC database did not include information on hemorrhagic lesions and amyloid-β presence was scored solely on a visual, categorical scale, a less specific variable compared to the AI generated continuous measures used in the MGH CAA cohort. It is possible that there are substantial differences in local CAA severity that was not detected because of the used methods. Secondly, as mentioned above, the sample size in the MGH CAA cohort was small. Moreover, it is a highly selected cohort, because the less affected hemisphere has been used for ex vivo MRI and histopathological analysis. This may have led to a relative under-representation of hemorrhagic MRI lesions. Via the statistical methods used in this paper, we aimed to correct for random effects. Despite this, we consider our study mainly exploratory, and our results need to be interpreted with care and should be replicated in larger cohorts. Thirdly, the use of autopsy data limits the observations to the final disease stage. Therefore, any sex differences which could have been present during life may no longer be seen in these data.[11] Lastly, by focusing solely on leptomeningeal grade III vessel remodelling, our methods may be more relevant in uncovering sex differences in cSS and ICH pathophysiology, whereas the implications for microhemorrhage pathophysiology warrants further investigation. Future studies need to investigate the effect of sex on parenchymal and grade IV vessel remodelling, although this is challenging as these vessels are rarely observed on routine neuropathological examination.

The results of this exploratory study suggest that, although sex may influence (parenchymal) amyloid-β accumulation and (factors contributing to) hemorrhage burden in CAA, the mechanisms behind these differences are complex and should be investigated in more detail in larger CAA cohorts. It is important to consider that the mechanisms might depend on (epi) genetic or environmental factors, or sex-specific hormones such as estrogen and testosterone. Future studies need to investigate sex-specific mechanisms that underlie the observed differences, as these could be possible targets for treatment or prevention in CAA.

Supplemental material

Supplemental results

Table 1: LME investigating sex differences in factors influencing cortical iron density, including outcomes without outlier.

	(0) M0	(1a) with leptomeningeal vessel remodelling	(1b) with leptomeningeal vessel remodelling interaction with sex	(2a) with leptomeningeal CAA area (%)	(2b) with leptomeningeal CAA area (%):sex	(3a) with cortical CAA area (%)	(3b) with cortical CAA area (%):sex	(4 comprehensive model
Age at death (y)	P=0.231 estimate= -0.541 (-1.412-0.432)[1]	P=0.143 estimate= -0.6241 (-1.468-0.218)	P=0.114 estimate= -0.649 (-1.458-0.159)	P=0.154 estimate= -0.640 (-1.525-0.255)	P=0.094 estimate= -0.740 (-1.596-0.135)	P=0.182 estimate= -0.577 (-13.108-3.392)	P=0.199 estimate= -0.522 (-1.331-0.2888)	P=0.111 estimate= -0.613 (-1.368-0.144)
	Without outlier: estimate: -0.43, p=0.19	Without outlier: estimate: -0.52, p=0.10	Without outlier: *estimate: -0.54,* *p=0.08*	Without outlier: estimate: -0.49, p=0.14	Without outlier: *estimate: -0.57,* *p=0.08*	Without outlier: estimate: -0.46, p=0.27	Without outlier: estimate: -0.41, p=0.16	Without outlier: *estimate: -0.5,* *p=0.08*
Sex (male 0, female 1)	P=0.473 estimate= -5.252 (-2.080-0.886)[1]	P=0.646 estimate= -3.147 (-17.012-10.728)	P=0.592 estimate= 4.437 (-12.391-20.779)	P=0.423 estimate= -5.667 (-19.876-8.667)	P=0.505 estimate= 9.272 (-19.172-36.698)	P=0.415 estimate= -5.687 (-19.679-8.476)	**P=0.038** **estimate= - 18.958** **(-36.549- - 0.832)**	P=0.102 estimate= -14.236 (-31.180-3.315)
	Without outlier: estimate: -3.8, p=0.47	Without outlier: estimate: -1.89, p=0.71	Without outlier: estimate: 4.67 p=0.43	Without outlier: estimate: -4.04, p=0.44	Without outlier: estimate: 7.15, p=0.48	Without outlier: estimate: -4.10, p=0.42	Without outlier: **estimate: -15.68,** **p=0.02**	Without outlier: *estimate: -11.12,* *p=0.07*
Leptomeningeal grade III vessel remodelling		**P=0.005** **estimate= 7.189** **(2.324-12.059)**	**P=0.002** **estimate= 9.735** **(3.853-15.618)**					**P=0.008** **estimate= 6.545** **(1.749-11.335)**
		Without outlier: **estimate: 6.63,** **p=0.00**	Without outlier: **estimate: 8.81** **p<0.01**					Without outlier: **estimate: 5.97,** **p<0.01**

	(0) M0	(1a) with leptomeningeal vessel remodelling	(1b) with leptomeningeal vessel remodelling interaction with sex	(2a) with leptomeningeal CAA area (%)	(2b) with leptomeningeal CAA area (%):sex	(3a) with cortical CAA area (%)	(3b) with cortical CAA area (%):sex	(4 comprehensive model
Leptomeningeal grade III vessel remodelling: sex			P=0.139 estimate= -7.686 (-18.034-2.609) Without outlier: estimate: -6.66 p=0.07					
Leptomeningeal CAA area (%)				P=0.299 estimate= 0.170 (-0.164-0.492) Without outlier: estimate: 0.1, p=0.42	P=0.115 estimate= 0.303 (-0.091-0.676) Without outlier: estimate: 0.2, p=0.16			
Leptomeningeal CAA area (%):sex					P=0.222 estimate= -0.434 (-1.133-0.287) Without outlier: estimate: -0.32, p=0.21			
Cortical CAA area (%)						P=0.235 estimate= -4.733 (-13.108-3.392) Without outlier: estimate: -3.25, p- 0.27	**P=0.022** **estimate= - 11.352** **(-21.378- -1.384)** **Without outlier:** **estimate: -9.00,** **p=0.01**	**P=0.028** **estimate= - 10.362** **(-20.040- - 0.752)** **Without outlier:** **estimate: -7.76,** **p=0.02**

	(0) M0	(1a) with leptomeningeal vessel remodelling	(1b) with leptomeningeal vessel remodelling interaction with sex	(2a) with leptomeningeal CAA area (%)	(2b) with leptomeningeal CAA area (%):sex	(3a) with cortical CAA area (%)	(3b) with cortical CAA area (%):sex	(4 comprehensive model
Cortical CAA area (%):sex							**P=0.034 estimate= 17.191 (1.351-33.279)**	*P=0.084 estimate= 13.516 (-1.97-29.276)*
							Without outlier: **estimate: 15.68, p=0.01**	Without outlier: **estimate: 11.31 p=0.04**
Log likelihood	-284.0	-279.9	-278.9	-283.5	-282.8	-283.4	-281	-278
AIC	580	574	573	581	582	580	578	573
BIC	593	589	591	597	599	596	596	593
Anova outcome (m0,…)		**0.004364**	0.141242	0.3066	0.2307	0.2521	**0.03377**	**0.005082**
		Without outlier **0.000258**	Without outlier *0.067600*	Without outlier 0.4223	Without outlier 0.2328	Without outlier 0.2941	Without outlier **0.01132**	Without outlier **0.0002784**

Results for the fixed effects of linear mixed effects models looking at the influence of sex on cortical iron density. Subject and cortical region (frontal, temporal, parietal, occipital) were set as random factors for the intercept. Data represent standardized fixed effects estimates with confidence intervals and statistical significance. Models were compared using likelihood ratio tests; smaller AIC and BIC values indicate a better model fit. Significant effects are highlighted in ***bold****, trend towards significance in italics. Results underlined are from LME ran without the outlier identified on the scatterplots (single section in a male subject).*
[1]95%CI obtained via bootstrapping.

References

1. Jäkel L, De Kort AM, Klijn CJM, Schreuder F, Verbeek MM. Prevalence of cerebral amyloid angiopathy: A systematic review and meta-analysis. Alzheimer's & dementia : the journal of the Alzheimer's Association 2022;18:10-28.
2. Charidimou A, Perosa V, Frosch MP, Scherlek AA, Greenberg SM, van Veluw SJ. Neuropathological correlates of cortical superficial siderosis in cerebral amyloid angiopathy. Brain : a journal of neurology 2020;143:3343-3351.
3. van Veluw SJ, Scherlek AA, Freeze WM, et al. Different microvascular alterations underlie microbleeds and microinfarcts. Annals of neurology 2019;86:279-292.
4. Koemans EA, Chhatwal JP, van Veluw SJ, et al. Progression of cerebral amyloid angiopathy: a pathophysiological framework. The Lancet Neurology 2023.
5. Vonsattel JP, Myers RH, Hedley-Whyte ET, Ropper AH, Bird ED, Richardson EP, Jr. Cerebral amyloid angiopathy without and with cerebral hemorrhages: a comparative histological study. Annals of neurology 1991;30:637-649.
6. Jäkel L, Van Nostrand WE, Nicoll JAR, Werring DJ, Verbeek MM. Animal models of cerebral amyloid angiopathy. Clin Sci (Lond) 2017;131:2469-2488.
7. Kozberg MG, Yi I, Freeze WM, et al. Blood–brain barrier leakage and perivascular inflammation in cerebral amyloid angiopathy. Brain Communications 2022;4.
8. Wermer MJH, Greenberg SM. The growing clinical spectrum of cerebral amyloid angiopathy. Current opinion in neurology 2018;31:28-35.
9. Charidimou A, Martinez-Ramirez S, Shoamanesh A, et al. Cerebral amyloid angiopathy with and without hemorrhage: evidence for different disease phenotypes. Neurology 2015;84:1206-1212.
10. Zhang-Nunes SX, Maat-Schieman ML, van Duinen SG, Roos RA, Frosch MP, Greenberg SM. The cerebral beta-amyloid angiopathies: hereditary and sporadic. Brain pathology (Zurich, Switzerland) 2006;16:30-39.
11. Koemans EA, Castello JP, Rasing I, et al. Sex Differences in Onset and Progression of Cerebral Amyloid Angiopathy. Stroke 2023;54:306-314.
12. Besser L, Kukull W, Knopman DS, et al. Version 3 of the National Alzheimer's Coordinating Center's Uniform Data Set. Alzheimer Disease & Associated Disorders 2018;32:351-358.
13. Olichney JM, Hansen LA, Lee JH, Hofstetter CR, Katzman R, Thal LJ. Relationship between severe amyloid angiopathy, apolipoprotein E genotype, and vascular lesions in Alzheimer's disease. Ann N Y Acad Sci 2000;903:138-143.
14. Thal DR, Rüb U, Orantes M, Braak H. Phases of A beta-deposition in the human brain and its relevance for the development of AD. Neurology 2002;58:1791-1800.
15. Kovacs GG, Gelpi E. Clinical neuropathology practice news 3-2012: the "ABC" in AD-revised and updated guideline for the neuropathologic assessment of Alzheimer's disease. Clin Neuropathol 2012;31:116-118.
16. Perosa V, Scherlek AA, Kozberg MG, et al. Deep learning assisted quantitative assessment of histopathological markers of Alzheimer's disease and cerebral amyloid angiopathy. Acta Neuropathol Commun 2021;9:141.
17. Auger CA, Perosa V, Greenberg SM, van Veluw SJ, Kozberg MG. Cortical superficial siderosis is associated with reactive astrogliosis in cerebral amyloid angiopathy. J Neuroinflammation 2023;20:195.

18. Wardlaw JM, Smith EE, Biessels GJ, et al. Neuroimaging standards for research into small vessel disease and its contribution to ageing and neurodegeneration. The Lancet Neurology 2013;12:822-838.
19. Perosa V, Oltmer J, Munting LP, et al. Perivascular space dilation is associated with vascular amyloid-β accumulation in the overlying cortex. Acta neuropathologica 2022;143:331-348.
20. Freeze WM, Bacskai BJ, Frosch MP, et al. Blood-Brain Barrier Leakage and Microvascular Lesions in Cerebral Amyloid Angiopathy. Stroke 2019;50:328-335.
21. Barnes LL, Wilson RS, Bienias JL, Schneider JA, Evans DA, Bennett DA. Sex differences in the clinical manifestations of Alzheimer disease pathology. Arch Gen Psychiatry 2005;62:685-691.
22. Oveisgharan S, Arvanitakis Z, Yu L, Farfel J, Schneider JA, Bennett DA. Sex differences in Alzheimer's disease and common neuropathologies of aging. Acta neuropathologica 2018;136:887-900.
23. Shinohara M, Murray ME, Frank RD, et al. Impact of sex and APOE4 on cerebral amyloid angiopathy in Alzheimer's disease. Acta neuropathologica 2016;132:225-234.
24. Cacciottolo M, Christensen A, Moser A, et al. The APOE4 allele shows opposite sex bias in microbleeds and Alzheimer's disease of humans and mice. Neurobiology of aging 2016;37:47-57.